Applied Surface Science 411 (2017) 331–337

Contents lists available at ScienceDirect

Applied Surface Science

journal homepage: www.elsevier.com/locate/apsusc

Full Length Article

Polyaniline (PANI) modified bentonite by plasma technique for U(VI) removal from aqueous solution

Xinghao Liu[a,b], Cheng Cheng[c], Chengjian Xiao[a,*], Dadong Shao[c,*], Zimu Xu[b,*], Jiaquan Wang[b], Shuheng Hu[b], Xiaolong Li[a], Weijuan Wang[a]

[a] Institute of Nuclear Physics and Chemistry, China Academy of Engineering Physics, Mianyang 621900, China
[b] Intelligent Manufacturing Technology Research Institute, Hefei University of Technology, Hefei 230088, China
[c] Institute of Plasma Physics, Chinese Academy of Sciences, Hefei 230031, China

ARTICLE INFO

Article history:
Received 21 January 2017
Received in revised form 3 March 2017
Accepted 9 March 2017
Available online 18 March 2017

Keywords:
Uranium
Bentonie
Adsorption
Polyaniline
Plasma technique

ABSTRACT

Polyaniline (PANI) modified bentonite (PANI/bentonie) was synthesized by plasma induced polymerization of aniline on bentonite surface, and applied to uptake of uranium(VI) ions from aqueous solution. The as-synthesized PANI/bentonie was characterized by scanning electron microscopy (SEM), powder X-ray diffraction (XRD), thermal gravimetric analysis (TGA), and X-ray photoelectron spectroscopy (XPS). Batch adsorption technique was utilized to investigate the adsorption of U(VI) on bentonite and PANI/bentonite. The adsorption of U(VI) (10 mg/L) on PANI/bentonite surface is fairly depend on solution pH, ionic strength, and temperature in solution. The modified PANI on PANI/bentonite surface significantly enhances its adsorption capability for U(VI). The presence of humic acid (HA) can sound enhance U(VI) adsorption on PANI/bentonite at pH < 6.5 because of the strong complexation, and inhibits U(VI) adsorption at pH > 6.5. According to the thermodynamic parameters, the adsorption of U(VI) on PANI/bentonite surface is a spontaneous and endothermic process. The results highlight the application of PANI/bentonite composites as candidate material for the uptake of trace U(VI) from aqueous solution.

1. Introduction

Uranium is a basic material of nuclear science and technique, and is a typical radioactive pollution due to its high toxicity and radioactivity. The major sources of uranium contaminants in environment are nuclear industrial, coal burning, milling of ores, and usage of fertilizers etc. [1,2]. For the public health and ecosystem safety, it is urgent to uptake uranium from environment, especially from aqueous solution. Many techniques, for instance ion-exchange processes [3], biological treatment [4], solvent extraction [5], surface complexation and adsorption [6–10], have been proposed and studied to remove U(VI) ions from solution. Notably, adsorption technique is widely used in the environment management in terms of characteristics including easy operation, low consumption, and high efficiency and environmentally friendly [11–17]. However, traditional adsorbents are usually surfing from low capability and/or high cost for tracing U(VI) in aqueous solution. Thereby, the design of efficient adsorbent with excellent adsorption capability is of great scientific challenges in nuclear science and technology.

Clay is a significant portion of environmental media which has an important influence on the migration of radionuclide in environmental solution. Among which, bentonite, a dioctahedral 2:1 clay mineral, includes many positive ions such as Cu^{2+}, Mg^{2+}, Na^{+}, and K^{+} are located in the structure and can be easily replaced by other ions during adsorption process [18,19]. However, the less surface functional groups greatly limit the application of bentonite in real work. To further enhance the adsorption capability of bentonite, we modified the surface of bentonite with polyaniline (PANI) aiming to utilize the strong affinity of the abound amine and imine groups in PANI with U(VI) [12].

In this work, PANI/bentonite with high adsorption efficiency for U(VI) was synthesized by plasma technique and well characterized. The effect of solution conditions on U(VI) adsorption onto PANI/bentonite surface were investigated by batch technique.

* Corresponding authors.
E-mail addresses: xiaocj@caep.cn (C. Xiao), shaodadong@126.com (D. Shao), xzm@mail.ustc.edu.cn (Z. Xu).

http://dx.doi.org/10.1016/j.apsusc.2017.03.095
0169-4332/

2. Experimental

2.1. Materials

The bentonite from Huangshan, Anhui Province was dispersed in 0.01 mol/L HCl solution to remove metal ions, and then washed with Milli-Q water and dried at 70 °C for 24 h. All other chemicals are in reagent grade. Milli-Q water was used in all experiments.

2.2. Preparation of PANI/bentonite

PANI/bentonite was synthesized by plasma induced polymerization of aniline on bentonite surface. Briefly, 2.0 g bentonite was pre-treated by air plasma for 30 min. The plasma treating power and air flow rate were 100 W and 10 mL/min, respectively. After air plasma treatment process, the treated bentonite materials were added into 50 mL aniline solution and reacted at 60 °C for 3 h. The resulted materials were separated and rinsed repeatedly with Milli-Q water and dried afterwards at 70 °C to obtain the PANI/bentonite composites. The colour of bentonite was gradually changed from yellowish white to reddish brown during the synthesis process. Meanwhile, The N_2-BET adsorption method surface area of bentonite and PANI/bentonite was determined to be 20.3 and 113.1 m^2/g, respectively. The increased surface area of PANI/bentonite is beneficial for the interaction of radionuclides.

2.3. Characterization

The physiochemical properties of bentonite and PANI/bentonite were measured and evaluated by XRD, TGA, XPS, and SEM techniques in detail. XRD patterns were recorded by X-ray diffraction (Rigaku D/max) with monochromatized Cu-Kα radiation. TGA curves were obtained by a Shimadzu TGA-50 thermo gravimetric analyzer at an air flow rate of 50 mL/min and the heating rate of 10 °C/min. XPS curves were obtained on an ESCALab220i-XL surface microanalysis system (VG Scientific) equipped with an Al Ka (hλ = 1486.6 eV) source. The SEM images were performed on a Sirion 200 SEM microscope.

2.4. Adsorption experiments

The adsorption efficiency of U(VI) was carried out by batch technique in polyethylene centrifuge tube. The stock PANI/bentonite and NaCl solution were added into the tube and pre-equilibrate for 12 h. After the desired amounts of U(VI) ($UO_2(NO_3)_2{\cdot}6H_2O$) were added, the solution pH was adjusted by adding negligible amounts of HCl or NaOH. The tubes were shaken for 24 h to ensure the adsorption equilibration, and then the adsorbents were separated by centrifugation (BECKMAN COULTER 64R) at 18,000 rpm for 15 min. The residual U(VI) concentration in supernatant was determined by Arsenazo III spectrophotometer. All adsorption data were the average of triplicate determinations and the relative errors were <5%.

3. Results and discussion

3.1. Characterization

The XRD patterns of raw bentonite and PANI/bentonite were shown in Fig. 1A, which is a technique to clarify the microscopic structures of bentonite and PANI/bentonite. According to the XRD peaks at 2θ = 6.04°, 19.86°, montmorillonite (M) is the dominant species of bentonite, and calcite (marked by C) and quartz (marked by Q) are also the important species in bentonite. The XRD peak 2θ = 62.00° (060) reflects the dioctahedral structure of bentonite [21]. On the basis of XRD data, natural bentonite and PANI/bentonite are fairly similar between 10° and 65°, which signifies that the structure of bentonite was not destroyed during plasma treatment process. The PANI/bentonite shows a new diffraction peak at 2θ = 9.06° [22] which confirms the successful modification of PANI on bentonite surface.

The TGA curves of bentonite and PANI/bentonite were shown in Fig. 1B. The weight losses related to moisture before 200 °C were ~1.49 and ~1.61% for raw bentonite and PANI/bentonite, respectively. In the high temperature, the weight losses can be due to the evaporation of physical and chemically absorbed water from galleries and chemical structure of bentonite [23,24], as well as the degradation and decomposition of PANI. The respective weight losses after 200 °C were ~5.85 and ~12.8% for raw bentonite and PANI/bentonite. According to TGA curve, the weigh percent of PANI in dry PANI/bentonite is ~6.92%.

XPS spectroscopy technique is used to study the functional groups on bentonite and PANI/bentonite surfaces. The C 1s spectra (Fig. 2A) of bentonite can be deconvoluted into five components at 284.5 ± 0.2, 285.2 ± 0.2, 286.2 ± 0.2, 287.2 ± 0.2 and 289.1 ± 0.2 eV, which are attributed to the sp^2-hybridized graphite-like C atoms (C═C), sp^3-hybridized C atoms (C—C), —C—O (i.e.g. alcohol and ether), —C═O (i.e. ketone and aldehyde), and —COOH (i.e. carboxylic and ester) species, respectively [25–27]. According to the quantitative analysis results of XPS C 1 s spectra of bentonite and PANI/bentonite (Table 1), the peak fractions of C═C and —COOH are increase and decrease after PANI modification, respectively. It reveals that PANI was modified on the surface of bentonite successfully, and parts —COOH was reduced by PANI in synthesis process [12]. The XPS O1s spectra of bentonite and PANI/bentonite can be deconvoluted into three peak components with binding energy at 531.8 ± 0.1, 532.6 ± 0.1 and 533.9 ± 0.1 eV, which are also assigned to —COO—, – C═O and —C—OH groups, respectively [28,29]. As shown in Fig. 2B and Table 2, the peak fraction of —COOH decreases, indicates the reduction of —COOH in synthesis process.

The SEM images of bentonite and PANI/bentonite are displayed in Fig. 3. The surface modification of PANI on bentonite surface induces remarkable alteration surface morphology. Raw bentonite (Fig. 3A and B) shows smooth surface with irregular shapes and aggregates together by inter-molecular forces [22,30]. After modification of PANI, the PANI/bentonite materials (Fig. 3C and D) display that the plate-like bentonite structures are encapsulated by PANI thin layer. The results of SEM images further confirm that PANI was modified on bentonite surface successfully.

3.2. Adsorption experiment

Effect of contact time on U(VI) adsorption on PANI/bentonite and on bentonite is depicted in Fig. 4A. The adsorptions of U(VI) onto PANI/bentonite and bentonite increase with increasing of contact time to 8 h, and then keep the level. Meanwhile, the adsorption of U(VI) on PANI/bentonite is higher than that on bentonite due to the effect of modified PANI on PANI/bentonite surface in terms of the strong affinity of U(VI) with the amine and imine groups in PANI [12]. In the following experiments, we select 24 h as the contact time to ensure the adsorption equilibrium. To study adsorption mechanisms, the kinetic data are simulated by pseudo-first-order kinetic models and pseudo-second-order kinetic models. Both linear formulas are expressed as follows [31,32]:

$$\ln(q_e - q_t) = \ln\ q_t - k_f * t \quad (1)$$

$$\frac{t}{q_t} = \frac{1}{k_s * q_e^2} + \frac{t}{q_e} \quad (2)$$

Where q_e (mg/g) and q_t (mg/g) are the adsorbed amounts U(VI) at equilibrium and contact time t, respectively. k_f and k_s present

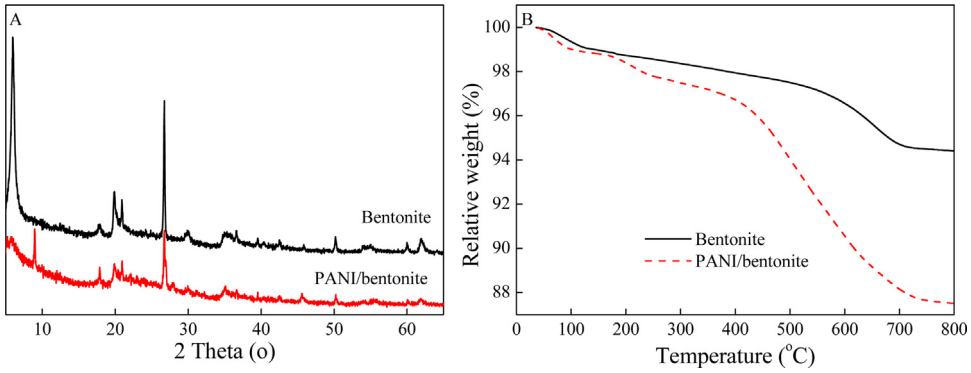

Fig. 1. XRD patterns (a) and TGA curves (b) of bentonite and PANI/bentonite.

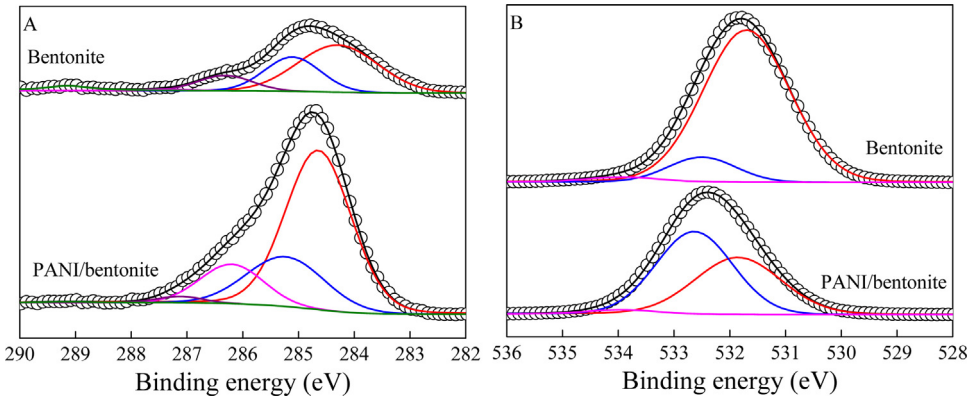

Fig. 2. XPS C1s (A) and O1s (B) spectra of bentonite and PANI/bentonite.

Table 1
Curve fitting results of XPS C 1s spectra.

	Peak	BE[a] (eV)	FWHM[b] (eV)	%
Bentonite	C═C	284.30	1.69	54.3
	C—C	285.11	1.18	27.7
	—C—OH	286.32	1.14	12.0
	>C═O	287.40	1.00	1.28
	—COOH	289.14	0.98	4.62
PANI/bentonite	C═C	284.64	1.39	62.2
	C—C	285.23	1.64	21.9
	—C—OH	286.20	1.33	14.2
	>C═O	287.12	0.94	1.58
	—COOH	289.10	1.00	0.14

[a] Binding energy.
[b] Full width at half-maximum.

Table 2
Curve fitting results of XPS O 1s spectra.

	Peak	BE (eV)	FWHM (eV)	%
Bentonite	—COOH	531.70	1.83	87.2
	>C═O	532.50	1.42	10.7
	—C—OH	533.93	1.45	2.09
PANI/bentonite	—COOH	531.83	1.82	43.2
	>C═O	532.64	1.62	54.6
	—C—OH	533.95	1.39	2.22

rate constants of the pseudo-first kinetic order model and pseudo-second order kinetic model, respectively.

As depicted in Fig. 4B, according to the correlation coefficient (R^2), the kinetic adsorption data can be better described by the pseudo-second order kinetic model, which indicates that the adsorption of U(VI) on PANI/bentonite surface is mainly controlled by chemisorption mechanism.

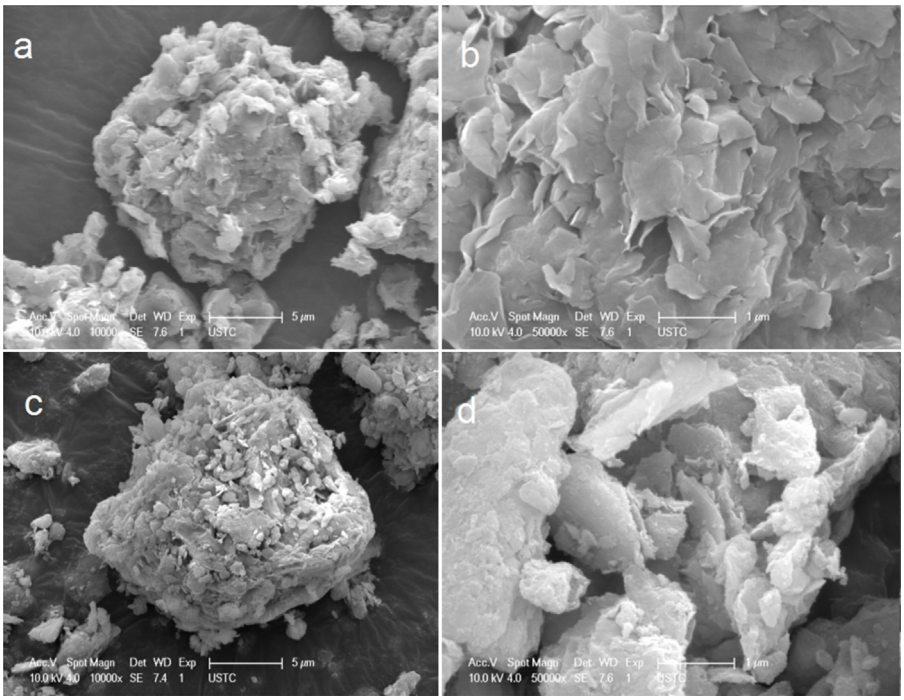

Fig. 3. SEM patterns of bentonite (a and b) and PANI/bentonite (c and d).

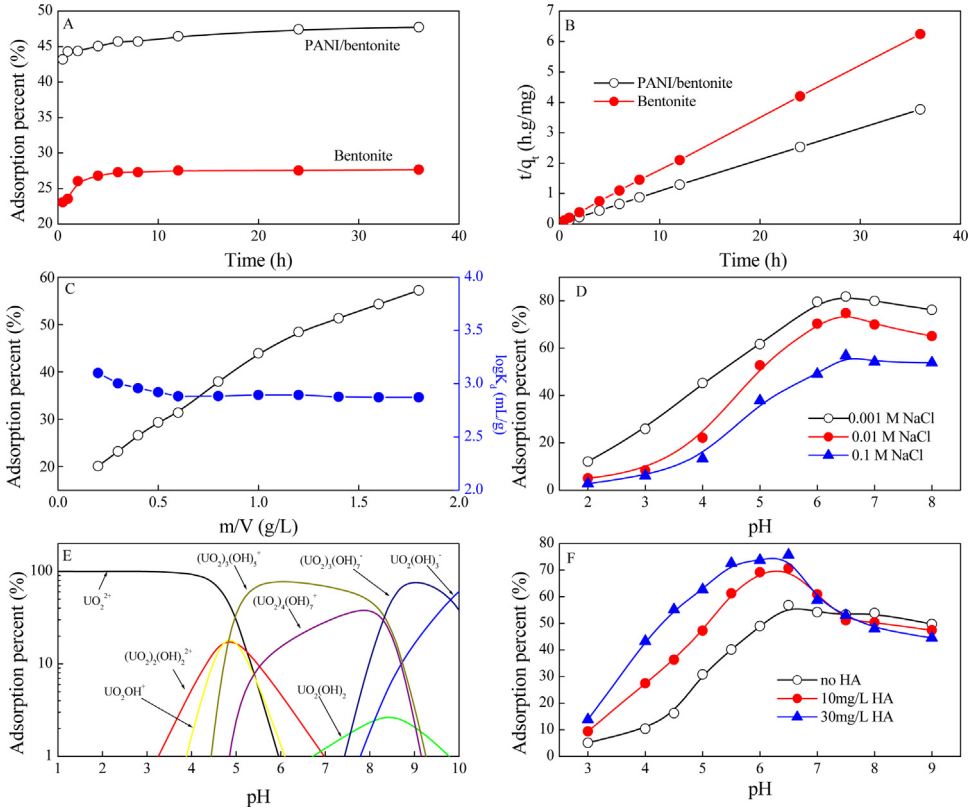

Fig. 4. Adsorption kinetics (A) and the fitting of pseudo-second order kinetic model (B) of U(VI) on PANI/bentonite and bentonite. pH 5.0 ± 0.1, T = 293 K, m/V = 0.5 g/L, $C[U(VI)]_{initial}$ = 10 mg/L, I = 0.1 mol/L NaCl. Effect of solid content on U(VI) adsorption on PANI/bentonite (C). pH = 5.0 ± 0.1, T = 293 K, C_0 = 10 mg/L, I = 0.1 mol/L NaCl. Effect of ionic strength on U(VI) adsorption to PANI/bentonite as a function of pH (D). m/V = 0.5 g/L, $C[U(VI)]_{initial}$ = 10 mg/L, I = 0.1, 0.01 and 0.001 mol/L NaCl, and T = 293 K. Relative proportion of 10 mg/L U(VI) species in solution as a function of pH values (E). The effect of pH on U(VI) adsorption to PANI/bentonite in the absence and presence of HA (F). pH = 5.0 ± 0.1, m/v = 0.5 g/L, T = 293 K, C_0 = 10 mg/L, I = 0.1 mol/L NaCl.

The distribution coefficient (K_d) as a function of PANI/bentonite are displayed in Fig. 4C. The K_d value is obtained by following equation:

$$K_d = \frac{C_s}{C_e} \quad (3)$$

With increasing adsorbent content, more surface sites [12] on PANI/bentonite surface are available for U(VI) binding and therefore increases U(VI) adsorption. As depicted in Fig. 4C, the adsorption efficiency of U(VI) on PANI/bentonite increases with the enhancing adsorbent content. Meanwhile, the competition among the functional groups on adsorbent surface would decrease the K_d value of U(VI) With increasing adsorbent content [33]. As depicted in Fig. 4C, K_d value of U(VI) adsorption gradually decreases with increasing adsorbent content, which can be explained by the competition of functional groups and reactive sites on PANI/bentonite for U(VI).

Solution pH has a sound influence on the adsorption of metal ions. The adsorption behavior of adsorbent toward metal ion depends on the protonation – deprotonation properties, so the adsorption behavior is greatly affected by solution pH. The effect of solution pH on U(VI) adsorption to PANI/bentonite was studied in three electrolyte concentrations (0.001, 0.01 and 0.1 mol/L NaCl) and shown in Fig. 4D. The adsorption of U(VI) increases abruptly at pH 4.0–6.5. The abrupt increase of U(VI) adsorption may be attributed to the surface precipitation of uranium on PANI/bentonite surface. At pH > 6.5, U(VI) adsorption decreases mainly due to the electrostatic repulsion. U(VI) exists as different species at different pH values. UO_2^{2+} is the dominant philosophy at pH < 4.0, and positive species ($UO_2(OH)^+$, $(UO_2)_3(OH)_5^+$, $(UO_2)_4(OH)_7^+$, $UO_2(OH)_2$) emerge at pH 4–7 [2,34,35]. At pH > 7, negatively charged U(VI) species are the dominant U(VI)species in solution.

As shown in Fig. 4D, the ionic strength is a fundamental factor which affects U(VI) adsorption on PANI/bentonite composites. It is also interesting to notice that adsorption of U(VI) on PANI/bentonite is obviously restrained by NaCl concentrations, which coincides with the results reported by Fan et al. [36]. The formed U(VI)-PANI/bentonite electric double layer complex can be enhanced when the concentration of the competing salt decreased. Solution ionic strength also affects the activity coefficient of ions in solution [37]. Ion exchange and/or outer-sphere surface complexation is usually considered as the main mechanism of adsorption, which can be expressed by the following reactions:

(1) Surface complexation:

$$\equiv SOH_2^+ + UO_2^{2+} \rightarrow \equiv SOHUO_2^+ + H^+ \quad (4)$$

$$2 \equiv SOH_2^+ + UO_2^{2+} \rightarrow (\equiv SOH)_2UO_2^{2+} + 2H^+ \quad (5)$$

$$\equiv SOH + UO_2^{2+} \rightarrow \equiv SOUO_2^+ + H^+ \quad (6)$$

$$2 \equiv SOH + UO_2^{2+} \rightarrow (\equiv SO)_2UO_2 + 2H^+ \quad (7)$$

(2) Exchange with Na ions:

$$\equiv SONa + UO_2^{2+} \rightarrow \equiv SOUO_2^+ + 2Na^+ \quad (8)$$

$$2 \equiv SONa + UO_2^{2+} \rightarrow (\equiv SO)_2UO_2 + 2Na^+ \quad (9)$$

(3) The hydrolysis of U(VI) in solution:

$$UO_2^{2+} + nH_2O \Leftrightarrow [UO_2(H_2O)_{n-m}]^{2-m} + mH^+ \quad (10)$$

Being n > m, and exchange with hydrolyzed species:

$$\equiv SOH + UO_2(OH)_m(H_2O)_{n-m}^{2-m} \Leftrightarrow \equiv SOUO_2(OH)_m^{1-m} + H^+ + (n-m)H_2O \quad (11)$$

Fig. 4F clearly shows that the increasing HA concentration enhances U(VI) adsorption on PANI/bentonite at pH < 6.5, while inhibits that at pH > 6.5, respectively. The enhanced U(VI) adsorption at low pH can be explained by the adsorption of negatively charged HA at the surface of PANI/bentonite. It reduces the positive surface charge and promotes the complexation of PANI/bentonite with U(VI) which forms PANI/bentonite-HA-U(VI). Furthermore, HA possesses abound functional groups which can form strong complex with U(VI), and thereby increases U(VI) adsorption on HA-bentonite hybrids. At higher pH, the surface of PANI/bentonite changes from positively charged to be negatively charged. The free and negatively-charged HA could easily complex with U(VI) in aqueous solution. This process competitively goes against the adsorption of U(VI) on PANI/bentonite [38].

Adsorption isotherms of U(VI) on PANI/bentonite surface at three different temperatures (293, 313, and 333 K) are shown in Fig. 5A. Obviously, U(VI) adsorption increased with increasing reaction temperature. To illustrate the adsorption mechanism, the Langmuir and the Freundlich isotherm models are used to simulate the adsorption isotherms. The Langmuir isotherm model is mainly used to elucidate the adsorption which occurs in a monolayer, which can be represented by the following equation:

$$C_s = \frac{bC_{s,\max}C_e}{1 + bC_e} \quad (12)$$

where C_e is the equilibrium concentration of U(VI) in supernatant; C_s is the amount of U(VI) adsorbed on per weight unit of adsorbent after equilibrium; $C_{s,max}$ is the maximum amount of U(VI) adsorbed at complete monolayer coverage; b is an adsorption constant.

The Freundlich isotherm model is used to describe the adsorption on heterogeneous surfaces, which can be described by the following form:

$$q_e = K_F C_e^{\,n} \quad (13)$$

The model can also be expressed as:

$$\log\ q_e = \log\ K_F + n \log\ c_e$$

Where K_F and n are the Freundlich constants representing the adsorption capability and adsorption intensity, respectively.

The model simulation results of adsorption isotherms are shown in Fig. 5B and C, and Table 3. The Langmuir model is found better to simulate the adsorption data which suggest that the adsorption of U(VI) on PANI/bentonite is in a monolayer coverage. The maximum adsorption capacities (C_{smax}) of U(VI) on PANI/bentonite surface calculated from the Langmuir model are 14.1, 16.2, and 17.5 mg/g at 293, 313, and 333 K under the experimental conditions, which are comparable to many adsorbent under similar experimental conditions, such as manganese oxide coated zeolite [39], natural clinoptilolite zeolite [40], natural white silica [41], and metal-organic framework [42].

The thermodynamic parameters (ΔG^0, ΔS^0 and ΔH^0) for U(VI) adsorption on PANI/bentonite are obtained from temperature dependent adsorption data.

The Gibbs free energy change (ΔG_0) is obtained from following relationship:

$$\Delta G^0 = -RT\ln K^0 \quad (15)$$

K^0 is thermodynamic equilibrium constant, and $\ln K^0$ values are calculated by plotting $\ln K_d$ as a function of C_e and extrapolating the C_e to zero. The values of ΔH^0 and ΔS^0 can be calculated from the relationship:

$$\ln\ K^0 = \frac{\Delta S^0}{R} - \frac{\Delta H^0}{RT} \quad (16)$$

$$\Delta S^0 = -\left(\frac{\partial \Delta G^0}{\partial T}\right)_P \quad (17)$$

The thermodynamic parameters (ΔG^0, ΔS^0, and ΔH^0) are shown in Table 4. The positive values of ΔH^0 suggest that the adsorption of U(VI) on PANI/bentonite surface is an endothermic process

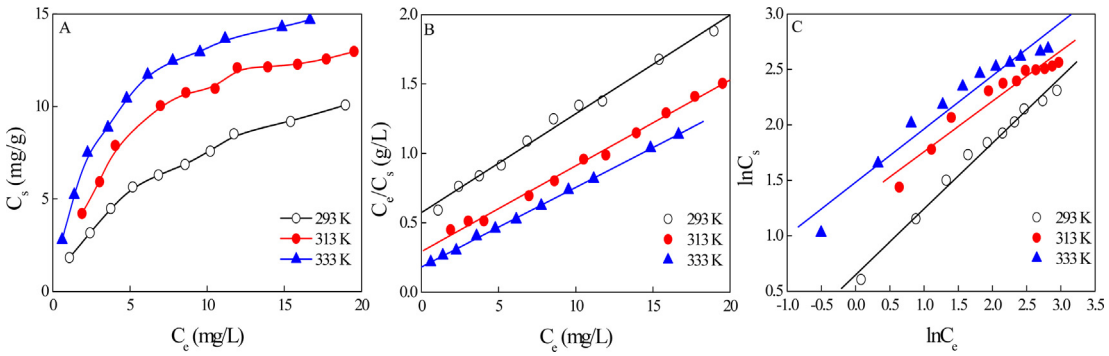

Fig. 5. Adsorption isotherms of U(VI) on PANI/bentonite at different temperatures (A). pH = 5.0 ± 0.1, m/V = 0.5 g/L, I = 0.1 mol/L NaCl. The Langmuir isotherm model (B) and the Freundlich isotherm model (C).

Table 3
Langmuir model and Freundlich models parameters for U(VI) adsorption at 293, 313, and 333 K.

T	Langmuir model			Freundlich model		
	$C_{s,max}$ (mg/g)	b (L/mg)	R^2	K_F (mg^{1-n} L^n/g)	n	R^2
293 K	14.1	0.124	0.991	1.91	0.594	0.985
313 K	16.2	0.211	0.994	3.68	0.455	0.935
333 K	17.5	0.314	0.999	4.41	0.481	0.948

Table 4
Thermodynamic parameters for U(VI) adsorption on PANI/bentonite.

T	$\triangle G^0$ (KJ/mol)	$\triangle H^0$ (KJ/mol)	$\triangle S^0$ (J/mol/K)
293 K	−18.5	20.2	131.2
313 K	−20.4		
333 K	−23.7		

and high temperature is in favor of U(VI) adsorption because the decomposition of U(VI) hydration sheath needs energy. The negative ΔG^0 value reveals a spontaneous process. With increasing temperature, the ΔG^0 becomes more negative. It indicates that more efficient adsorption might happen at higher temperatures. The thermodynamic parameters indicate that the adsorption of U(VI) on PANI/bentonite surface is a spontaneous and endothermic process.

The regeneration-reuse property of PANI/bentonite is important for its real application. In this paper, the reusability of PANI/bentonite was studied by rinsing U-laden PANI/bentonite with 0.1 mol/L HCl and rinsed with Milli-Q water thoroughly. As depicted in Fig. 6, even after (at least) seven cycles of applications, the regenerated PANI/bentonite still presents similar adsorption capacity for U(VI) as compared with raw PANI/bentonite, which reveals that PANI/bentonite has excellent stability and can be used as regenerated availability adsorbent in potential application.

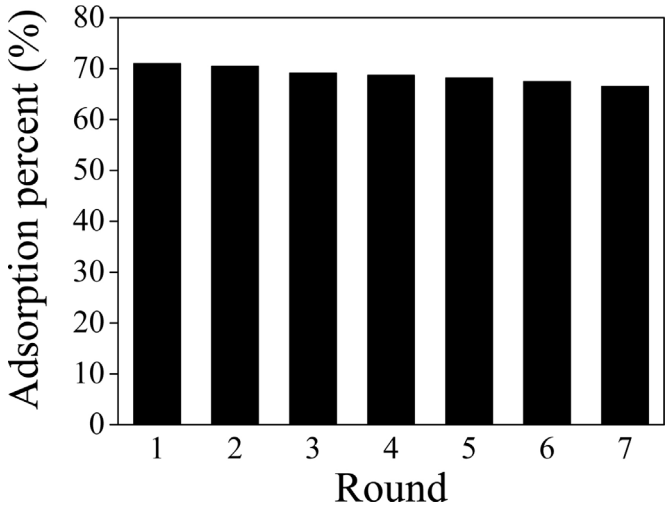

Fig. 6. Recycling of PANI/bentonite in extraction of U(VI) from aqueous solutions. T = 293 ± 1 K, $C[U(VI)]_{initial}$ = 10.0 mg/L, m/V = 0.5 g/L, pH = 5.0 ± 0.1, C[NaCl] = 0.01 mol/L.

4. Conclusion

PANI/bentonite was successfully synthesized by plasma technique in this work. The adsorption of U(VI) on PANI/bentonite surface is a spontaneous and endothermic process, which followed pseudo second order kinetics models and can be well described by the Langmuir models. Moreover, the adsorption process is depend on the solution pH and ionic strength. The HA in solution has a significant effect the adsorption efficiency.

Acknowledgments

Financial supports from the NSAF (U1530131), the National Natural Science Foundation of China (11675210, 51541807), the Radiochemistry 909 Project in the China Academy of Engineering Physics, the Science and Technology Development Foundation of China Academy of Engineering Physics (2014B0301034), and the China Postdoctoral Science Foundation (2015M582769XB, 2016T90872) are acknowledged.

References

[1] Y. Zhang, Y. Li, X. Zheng, Removal of atrazine by nanoscale zero valent iron supported on organobenton, Sci. Total Environ. 409 (2011) 625–630.
[2] D. Shao, Z. Jiang, X. Wang, J. Li, Y. Meng, Plasma induced grafting carboxymethyl cellulose on multiwalled carbon nanotubes for the removal of UO_2^{2+} from aqueous solution, J. Phys. Chem. B 113 (2009) 860–864.
[3] C. Banerjee, N. Dudwadkar, S.C. Tripathi, P.M. Gandhi, V. Grover, C.P. Kaushik, A.K. Tyagi, Nano-cerium vanadate a novel inorganic ion exchanger for removal of americium and uranium from simulated aqueous nuclear waste, J. Hazard. Mater. 280 (2014) 63–70.
[4] D.R. Lovley, E.J.P. Phillips, Y.A. Gorby, E.R. Linda, Microbial reduction of uranium, Nature 350 (1991) 413–416.
[5] L. Yuan, M. Sun, X. Liao, Y. Zhao, Z. Chai, W. Shi, Solvent extraction of U(VI) by trioctylphosphine oxide using a room-temperature ionic liquid, Sci. China Chem. 57 (2014) 1432–1438.

[6] Q. Jin, L. Su, G. Montavon, Y. Sun, Z. Chen, Surface complexation modeling of U(VI) adsorption on granite at ambient/elevated temperature: experimental and XPS study, Chem. Geol. 433 (2016) 81–91.
[7] H. Zhao, X. Liu, M. Yu, Z. Wang, B. Zhang, H. Ma, M. Wang, J. Li, A study on the degree of amidoximation of polyacrylonitrile fibers and its effect on their capacity to adsorb uranyl ions, Ind. Eng. Chem. Res. 12 (2015) 3101–3106.
[8] H. Liu, R. Wang, H. Jiang, H. Gong, X. Wu, Study on adsorption characteristics of uranyl ions from aqueous solutions using zirconium hydroxide, J. Radioanal. Nucl. Chem. 308 (2016) 213–220.
[9] X. Yang, J. Li, T. Wen, X. Ren, Y. Huang, X. Wang, Adsorption of naphthalene and its derivatives on magnetic graphene composites and the mechanism investigation, Colloid Surf. A 422 (2013) 118–125.
[10] J. Li, Z. Guo, S. Zhang, X. Wang, Enrich and seal radionuclides in magnetic agarose microspheres, Chem. Eng. J. 172 (2011) 892–897.
[11] B. Buszewski, M. Szultka, Past, present, and future of solid phase extraction: a review, Crit. Rev. Anal. Chem. 42 (2012) 198–213.
[12] D. Shao, G. Hou, J. Li, T. Wen, X. Ren, X. Wang, PANI/GO as a super adsorbent for the selective adsorption of uranium(VI), Chem. Eng. J. 255 (2014) 604–612.
[13] D.G. Strawn, D.L. Sparks, The use of XAFS to distinguish between inner-and outer-sphere lead adsorption complexes on montmorillonite, J. Colloid Interface Sci. 216 (1999) 257–269.
[14] B. Petriea, R. Bardenb, B. Kasprzyk-Horderna, A review on emerging contaminants in wastewaters and the environment: current knowledge, understudied areas and recommendations for future monitoring, Water Res. 72 (2015) 3–27.
[15] S. Wang, M. Ma, W. Man, Q. Zhang, X. Niu, G. Sun, W. Zhang, T. Jiao, One-step facile fabrication of sea urchin-like zirconium oxide for efficient phosphate sequestration, RSC Adv. 5 (2015) 91218–91224.
[16] Y. Wan, Z. Zhang, Y. Liu, X. Cao, Adsorption of U(VI) from aqueous solution by the carboxyl-mesoporous carbon, Chem. Eng. J. 198–199 (2012) 246–-.
[17] W. Li, X. Han, X. Wang, Y. Wang, W. Wang, H. Xu, T. Tan, W. Wu, H. Zhang, Recovery of uranyl from aqueous solutions using amidoximated polyacrylonitrile/exfoliated Na-montmorillonite composite, Chem. Eng. J. 279 (2015) 735–746.
[18] A.S. Özcan, A. Özcan, Adsorption of acid dyes from aqueous solutions onto acid-activated bentonite, J. Colloid Interface Sci. 276 (2004) 39–46.
[19] T.S. Anirudhan, M. Ramachandran, Adsorptive removal of basic dyes from aqueous solutions by surfactant modified bentonite clay (organoclay): kinetic and competitive adsorption isotherm, Process Saf. Environ. Prot. 95 (2015) 215–225.
[21] J. Xiao, Y. Chen, W. Zhao, J. Xu, Sorption behavior of U(VI) onto Chinese bentonite: effect of pH ionic strength, temperature and humic acid, J. Mol. Liq. 188 (2013) 178–185.
[22] K. Wu, T. Ting, G. Wang, W. Ho, C.C. Shih, Effect of carbon black content on electrical and microwave absorbing properties of polyaniline/carbon black nanocomposites, Polym. Degrad. Stab. 93 (2008) 483–488.
[23] C. Vipulanandan, A. Mohammed, Effect of nanoclay on the electrical resistivity and rheological properties of smart and sensing bentonite drilling muds, J. Pet. Sci. Eng. 130 (2015) 86–95.
[24] G. Liu, W. Guo, M. Pei, F. Meng, L. Wang, Synthesis of bentonite grafted by cationic polymer for the adsorption of amido black 10B, Colloid Polym. Sci. 294 (2016) 2005–2012.
[25] D. Shao, J. Hu, X. Wang, Plasma induced grafting multiwalled carbon nanotube with chitosan and its application for removal of UO_2^{2+} Cu^{2+}, and Pb^{2+} from aqueous solutions, Plasma Process. Polym. 7 (2010) 977–985.
[26] B. Qiu, C. Xu, D. Sun, H. Wei, X. Zhang, J. Guo, Q. Wang, Z. Guo, S. Wei, Polyaniline coating on carbon fiber fabrics for improved hexavalent chromium removal, RSC Adv. 4 (2014) 29855–29865.
[27] B. Mu, W. Zhang, S. Shao, A. Wang, Glycol assisted synthesis of graphene–MnO_2–polyaniline ternary composites for high performance supercapacitor electrodes, Phys. Chem. Chem. Phys. 16 (2014) 7872–7880.
[28] C. Tao, J. Wang, S. Qin, Y. Lv, Y. Long, H. Zhu, Z. Jiang, Fabrication of pH-sensitive graphene oxide–drug supramolecular hydrogels as controlled release systems, J. Mater. Chem. 22 (2012) 2486–2856.
[29] B. Yu, X. Wang, X. Qian, W. Xing, H. Yang, Functionalized graphene oxide/phosphoramide oligomer hybrids flame retardant prepared via in situ polymerization for improving the fire safety of polypropylene, RSC Adv. 4 (2014) 31782–31794.
[30] R.R. Tiwari, K.C. Khilar, U. Natarajan, Synthesis and characterization of novel organo-montmorillonites, Appl. Clay Sci. 38 (2008) 203–208.
[31] R. Sabyasachi, K. Ajay, R.P. Mana, T.R. Mangal, Pseudo second order kinetic model for the sorption of U(VI) onto soil: a comparison of linear and non-linear methods, Int. J. Environ. Sci. 6 (2015) 145–154.
[32] Y. Zhao, J. Li, L. Zhao, S. Zhang, Y. Huang, X. Wu, X. Wang, Synthesis of amidoxime-functionalized Fe_3O_4@SiO_2 core–shell magnetic microspheres for highly efficient sorption of U(VI), Chem. Eng. J. 235 (2014) 275–283.
[33] K. Bhattacharyya, S. Gupta, Adsorption of Fe(III), Co(II) and Ni(II) on ZrO-kaolinite and ZrO-montmorillonite surfaces in aqueous medium, Colloid Surf. A 317 (2008) 71–79.
[34] D. Shao, X. Wang, J. Li, Y. Huang, X. Ren, G. Hou, X. Wang, Reductive immobilization of uranium by PAAM–FeS/Fe_3O_4 magnetic composites, Environ. Sci. Water Res. 1 (2015) 169–176.
[35] D. Shao, X. Wang, X. Wang, S. Hu, T. Hayat, A. Alsaedi, J. Li, S. Wang, J. Hu, X. Wang, Zero valent iron/poly(amidoxime) adsorbent for the separation and reduction of U(VI), RSC Adv. 6 (2016) 52076–52081.
[36] J. Zhang, A. Wang, Adsorption of Pb(II) from aqueous solution by chitosan-g-poly(acrylic acid)/attapulgite/sodium humate composite hydrogels, Chem. Eng. Data 55 (2010) 2379–2384.
[37] Z. Reddad, C. Gerente, Y. Andres, L.P. Cloirec, Adsorption of several metal ions onto a low-cost biosorbent: kinetic and equilibrium studies, Environ. Sci. Technol. 36 (2002) 2067–2073.
[38] H. Geckeis, T. Rabung, T.N. Manh, J. Kim, H. Beck, Humic colloid borne nature polyvalent metal ions: dissociation experiment, Environ. Sci. Technol. 36 (2002) 2946–2952.
[39] R. Han, W. Zou, Y. Wang, L. Zhu, Removal of uranium(VI) from aqueous solutions by manganese oxide coated zeolite: discussion of adsorption isotherms and pH effect, J. Environ. Radioact. 93 (2007) 127–143.
[40] L. Camacho, S. Deng, R.R. Parr, Uranium removal from groundwater by natural clinoptilolite zeolite: effects of pH and initial feed concentration, J. Hazard. Mater. 175 (2010) 393–398.
[41] A.A. El-Bayaa, N.A. Badawy, A.M. Gamal, I.H. Zidan, A.R. Mowafy, Purification of wet process phosphoric acid by decreasing iron and uranium using white silica sand, J. Hazard. Mater. 190 (2011) 324–329.
[42] J. Li, L. Gong, X. Feng, L. Zhang, H. Wu, C. Yan, Y. Xiong, H. Gao, F. Luo, Direct extraction of U(VI) from alkaline solution and seawater via anion exchange by metal-organic framework, Chem. Eng. J. 316 (2017) 154–159.